An Evaluation of Lysyl Oxidase–Derived Cross-Linking in Keratoconus by Liquid Chromatography/Mass Spectrometry

Anna Takaoka,[1] Natasha Babar,[1] Julia Hogan,[1] MiJung Kim,[1] Marianne O. Price,[2] Francis W. Price Jr,[3] Stephen L. Trokel,[1] and David C. Paik[1]

[1]Department of Ophthalmology, Columbia University College of Physicians and Surgeons, New York, New York, United States
[2]The Cornea Research Foundation of America, Indianapolis, Indiana, United States
[3]Price Vision Group, Indianapolis, Indiana, United States

Correspondence: David C. Paik, Department of Ophthalmology, Edward S. Harkness Eye Institute, Columbia University, College of Physicians and Surgeons, 160 Fort Washington Avenue, Room 715, New York, NY 10032, USA;
dcp14@columbia.edu.

Submitted: September 2, 2015
Accepted: November 19, 2015

Citation: Takaoka A, Babar N, Hogan J, et al. An evaluation of lysyl oxidase–derived cross-linking in keratoconus by liquid chromatography/mass spectrometry. *Invest Ophthalmol Vis Sci*. 2016;57:126–136. DOI:10.1167/iovs.15-18105

Purpose. Current literature contains scant information regarding the extent of enzymatic collagen cross-linking in the keratoconus (KC) cornea. The aim of the present study was to examine levels of enzymatic lysyl oxidase–derived cross-links in stromal collagen in KC tissue, and to correlate the cross-link levels with collagen fibril stability as determined by thermal denaturation temperature (T_m).

Methods. Surgical KC samples ($n = 17$) and Eye-Bank control ($n = 11$) corneas of age 18 to 68 years were analyzed. The samples were defatted, reduced ($NaBH_4$), hydrolyzed (6N HCl at 110°C for 18 hours), and cellulose enriched before analysis by C8 high-performance liquid chromatography equipped with parallel fluorescent and mass detectors in selective ion monitoring mode (20 mM heptafluorobutyric acid/methanol 70:30 isocratic at 1 mL/min). Nine different cross-links were measured, and the cross-link density was determined relative to collagen content (determined colorimetrically). The T_m was determined by differential scanning calorimetry.

Results. Cross-links detected were dihydroxylysinonorleucine (DHLNL), hydroxylysinonorleucine, lysinonorleucine (LNL), and histidinohydroxylysinonorleucine in both control and KC samples. Higher DHLNL levels were detected in KC, whereas the dominant cross-link, LNL, was decreased in KC samples. Decreased LNL levels were observed among KC $\leq$ 40 corneas. There was no difference in total cross-link density between KC samples and the controls. Pyridinolines, desmosines, and pentosidine were not detected. There was no notable correlation between cross-link levels with fibril instability as determined by T_m.

Conclusions. Lower levels of LNL in the KC cornea suggest that there might be a cross-linking defect either in fibrillar collagen or the microfibrillar elastic network composed of fibrillin.

Keywords: cornea, sclera, tissue cross-linking, keratoconus, progressive myopia

Riboflavin/UV-A photochemical corneal cross-linking (i.e., CXL) has revolutionized the field of corneal therapeutics. In just over 15 years this new treatment option for keratoconus (KC) and post-LASIK keratectasia has gone from a laboratory experiment to standard of care throughout the world. Increasing mechanical tissue strength, through the induction of covalent cross-linking in the corneal stroma, using the CXL method, can effectively halt the progression of KC.[1] Although a substantial body of literature has accrued in recent years regarding the CXL procedure as a treatment for KC, we still know very little about the possible cross-linking alterations that underlie the disease. In other words, there is scant information available regarding the enzymatic cross-linking that "pre-exists" (or may exist in an altered form) in the diseased keratoconic cornea.

The term "cross-linking" implies the introduction of new covalent bonds between amino acid residues in collagen molecules at the level of the fibril and can occur via enzymatic and nonenzymatic means. The enzymatic process is a well-regulated precise mechanism that results in the modification of very specific sites along the collagen primary chain.[2–4] Nonenzymatic cross-linking mechanisms include any means of introducing covalent bonds without using enzyme catalysts and includes riboflavin photochemistry (i.e., CXL) and chemical cross-linking agents such as glutaraldehyde, formaldehyde, genipin, glycating agents (such as ribose, glucose, and glyceraldehyde), and formaldehyde releasers (such as nitro-alcohols and sodium hydroxymethylglycinate). The reactions occurring with these nonenzyamtic mechanisms are more random or adventitious and can result in a variety of cross-link and non–cross-link (i.e., adduct) products, such as dityrosine in the case of CXL[5] and photooxidation of the lens,[6] and pentosidine[7] in the case of nonenzymatic glycation.

Under physiological conditions, collagen molecules assemble into fibrils that can then undergo an enzymatic posttranslational modification in the extracellular space that results in fibril stabilization (i.e., maturation) through enzymatic collagen cross-linking. This occurs through the action of the enzyme lysyl oxidase (i.e., protein-6-oxidase or LOX) and its related LOX-like enzymes (LOXL-1 to LOXL-4).[8–10] In this way, the

collagen fibrils attain their hallmark tensile strength and stability and tissue-specific elastic properties. LOX transforms the ε-amino groups of certain lysines and hydroxylysines into aldehyde groups through an oxidative deamination. These newly formed aldehydes can then spontaneously react with a second ε-amino group of lysine/hydroxylysine, in proximity, to create a Schiff base as an aldimine or keto-imine, which further reacts to form difunctional lysine- and hydroxylysine-derived cross-links.[11,12]

Recent genetic[13] and immunohistochemistry[14] studies have implicated LOX, the enzyme responsible for enzymatic collagen cross-linking, in the pathogenesis of KC. Two genetic variants at single nucleotide polymorphisms rs10519694 and rs2956540 located in intron 4 have been confirmed recently.[15] Further supporting a role for a cross-linking defect in KC, using immunohistochemistry, levels of LOX, as well as LOXL-1 and LOXL-3, have been reported as diminished in KC specimens[14] (Dudakova L, et al. *IOVS* 2013;54:ARVO E-Abstract 5293).

Pathologically, the keratoconic cornea displays several features that may be attributable to collagen enzymatic cross-link alterations, including changes in the distribution of collagen fibril diameters. As the disease progresses, the proportion of both very small and larger diameter fibrils increases, becoming particularly conspicuous in severe disease in all corneal layers.[16] Similar changes can be induced in animals through the use of LOX inhibitors such as β-aminopropionitrile,[17] a well-known agent for inducing lathyrism in animals and humans. As well, breaks (fractures) in Bowman's membrane have been described as one of the earliest findings by scanning electron microscopy,[18] and other abnormalities of the KC extracellular matrix have been reported.[19,20] The collagen extractability in KC has also been shown to be increased, consistent with diminished cross-linking.[21]

From a chemical cross-link perspective, the cornea is unique from most other collagenous tissues in that trifunctional histidine-based collagen cross-links are formed,[11] similar to skin.[12] The degree of hydroxylation can also vary and result in different di- and trifunctional cross-links.[2–4] Difunctional lysine- and hydroxylysine-derived cross-links are the initial compounds formed enzymatically through the action of LOX in the extracellular environment during the fibril stabilization/maturation process.[9,10] The subsequent development of the trifunctional histidine-based cross-link, histidinohydroxylysinonorleucine (HHL), occurs spontaneously across a Schiff base.[11]

Surprisingly, the only previous attempts to elucidate corneal collagen enzymatic cross-links (i.e., LOX mediated) in KC were performed before 1988, using traditional HPLC techniques for difunctional enzymatic cross-link analysis.[22–24] Regarding CXL, few studies have examined the specific chemical cross-links formed in the treated tissues,[25] although dityrosine has been detected as a cross-link product of riboflavin photochemical modification of collagen types I and IV in vitro[26] and its presence has been suggested in a recent rabbit study using total sample fluorescence.[5]

Traditional methods of difunctional cross-link analysis use tritiated sodium borohydride ($NaB[^3H]_4$) and other pre- or postcolumn derivatization methods. The trifunctional cross-link HHL has been measured by using postcolumn derivatization methods and the trifunctional pyridinolines and advanced glycation end-product cross-link pentosidine (Pent), by using native fluorescence. The mass spectrum detector (MSD) allows us to measure all of these cross-links simultaneously and with improved sensitivity over existing fluorescence methods. In the present study, we adopted a liquid chromatography/mass spectrometry (LC/MS) method that has recently been reported in studies related to bone and tendon.[27]

Thus, the current study was undertaken in order to measure levels of three difunctional (dihydroxylysinonorleucine, hydroxylysinonorleucine, and lysinonorleucine [LNL]) and three trifunctional enzymatic collagen cross-links (HHL, pyridinoline, and deoxypyridinoline), two elastin tetrafunctional cross-links (desmosine and isodesmosine), and the age-related nonenzymatic glycation difunctional cross-link (Pent) (Fig. 1A). The analysis was carried out in conjunction with an evaluation of collagen fibril thermal denaturation temperature (T_m) by differential scanning calorimetry (DSC). The results indicated that LNL is the dominant difunctional cross-link in the human cornea and its level is lower in KC samples than controls.

Materials and Methods

Corneal Samples

The research followed the tenets of the Declaration of Helsinki. Human donor control corneas (age 18–58 years) were obtained from the Eye-Bank for Sight Restoration, New York, New York. Surgical KC specimens (age 22–68 years) were obtained at the time of corneal transplant from patients undergoing anterior lamellar keratoplasty (ALK), deep anterior lamellar keratoplasty (DALK), and penetrating keratoplasty (PKP) through an ongoing clinical collaboration and with informed consent. Samples were divided into two age groups: $\leq$40 years and $>$40 years. Sample numbers (n) for control $\leq$ 40 was $n = 5$; control $>$ 40, $n = 6$; KC $\leq$ 40, $n = 8$; and KC $>$ 40, $n = 9$.

Chemical Reagents

Liquid chromatography/MS–grade methanol was purchased from VWR (Randor, PA, USA). The following reagents were purchased from Sigma-Aldrich Corp. (St. Louis, MO, USA): ion chromatography–grade heptafluorobutyric acid (HFBA), analytic-grade 6N hydrochloric acid (HCl), sodium borohydride ($NaBH_4$), sodium hydroxide, HPLC-grade butanol, HPLC-grade 1-propanol, sodium acetate trihydrate, citric acid monohydrate, glacial acetic acid (AcOH), Chloramine-T, dimethylaminobenzaldehyde, ACS-grade perchloric acid, HPLC-grade acetonitrile (ACN), and L-hydroxyproline (OH-pro). Necessary standards for collagen cross-link analysis were obtained from various sources. Dihydroxylysinonorleucine (DHLNL) and LNL were purchased from Santa Cruz Biotechnology, Inc. (Dallas, TX, USA). Pyridinoline (PYD)/deoxypyridinoline (DPYD) HPLC calibrator was purchased from Quidel Corp. (San Diego, CA, USA) and Pent was purchased from Cayman Chemical (Ann Arbor, MI, USA). The elastin cross-links desmosine (DES) and isodesmosine (IDE) were also commercially available from MP Biomedicals (Santa Ana, CA, USA). We also obtained as a kind gift from Simon P. Robins (University of Aberdeen, Aberdeen, Scotland, UK), the major trifunctional corneal cross-link HHL as well as the difunctional cross-link hydroxylysinonorleucine (HLNL).

Differential Scanning Calorimetry

A 6-mm trephine punch provided approximately 20 mg human cornea, which was sufficient mass for DSC analysis. The weight of the KC specimens varied between 5 to 20 mg, depending on the size and the thickness. (Amounts below 2 mg have smaller signal-to-noise ratios and can complicate thermogram peak analysis.) The samples were rinsed in bathing solution containing antiprotease, antimicrobial solution containing 1 mM EDTA and penicillin/streptomycin. Tissue samples were carefully blotted in a standardized, repetitive manner on a double-folded paper towel to remove excess solution/Dulbecco's phosphate-buffered saline and transferred to preweighed 50-μL aluminum pans. (Residual water in the pan can shift the thermogram downward, since water has a high heat capacity.) The samples

Investigative Ophthalmology & Visual Science

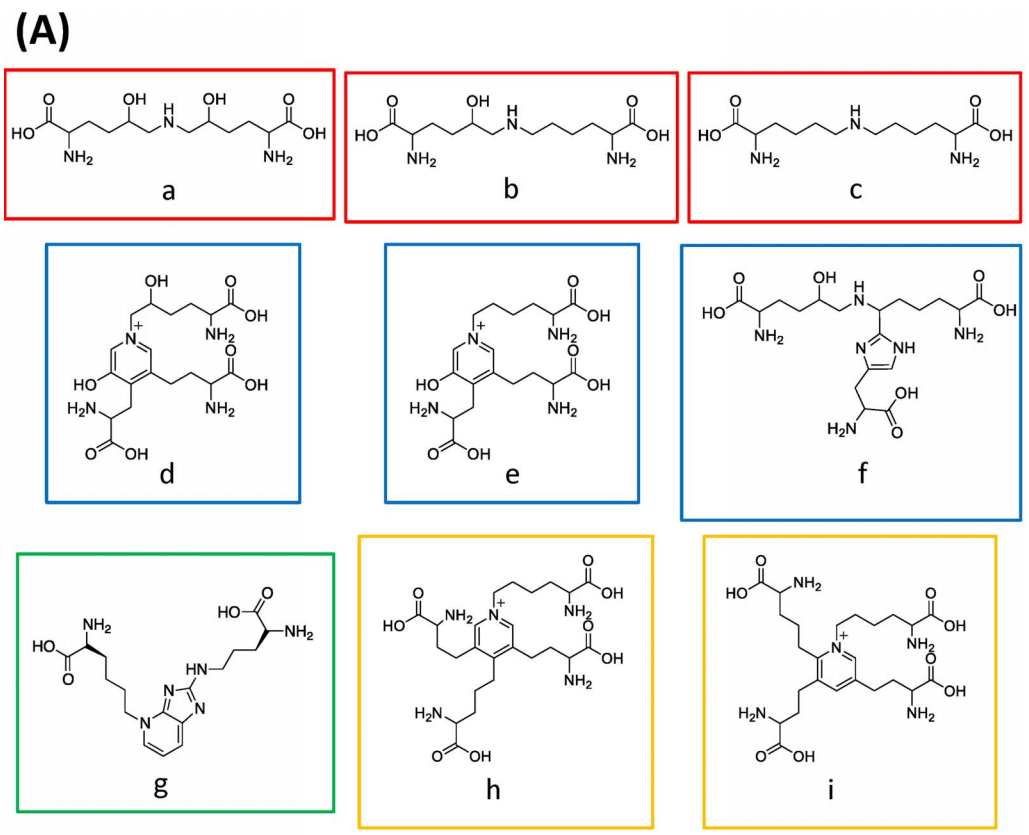

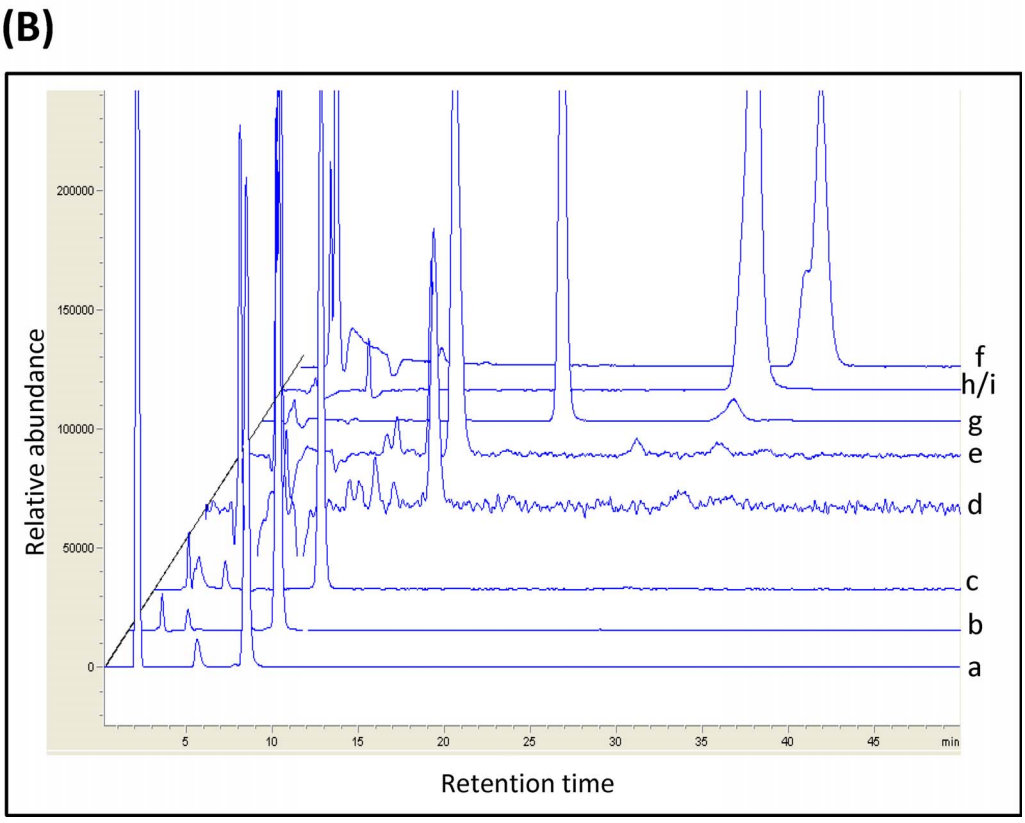

Figure 1. (**A**) Structures of important human corneal CTP di-, tri-, and tetrafunctional cross-links measured in this study. On the top line (*red boxes*) are the difunctional cross-links (**a**) DHLNL ($m/z = 308.2$), (**b**) HLNL ($m/z = 292.2$), and (**c**) LNL ($m/z = 276.1$). On the middle line (*blue boxes*) are the trifunctional cross-links (**d**) PYD ($m/z = 429.2$), (**e**) DPYD ($m/z = 413$), and (**f**) HHL ($m/z = 445.2$). On the *bottom line* are the age-related difunctional cross-link (*green box*) (**g**) Pent ($m/z = 379.2$) and the tetrafunctional elastin cross-links (*yellow boxes*) (**h**) DES ($m/z = 526.3$) and (**i**) IDE ($m/z = 526.3$). (**B**) The CTP cross-link elution profile using LC/MS overlaid extracted ion chromatograms from nine different cross-links (**a**–**i**). See Materials and Methods for details of the chromatographic separation procedure. CTP, connective tissue protein.

Investigative Ophthalmology & Visual Science

were flattened onto the bottom of the pan to ensure uniform heat transfer from the pan to the tissue and reduce the margin of error in the readings. The pans were immediately hermetically sealed by using a DSC pan-sealing press (Perkin-Elmer Universal Crimper Press; Perkin-Elmer, Waltham, MA, USA), which is used to prevent tissue dehydration from evaporation, and loaded into the DSC autosampler.

Thermal denaturation temperature of all samples was measured by using a Perkin-Elmer DSC 6000 autosampler and Pyris software (version 11.0). The samples were heated from 40°C to 70°C at a scan speed of 1°C/min, which was determined to be an optimal scan speed from preliminary runs. Denaturation curves representing differential heat flow over time were generated. The DSC heat flow endotherm data were then analyzed by interpolation of a segment of the curve containing the major endotherm. The maximal transition temperature point was identified by using the Pyris data analysis peak search function. The instrument has an expected margin of error of ±0.3°C, based on calibration runs, and is consistent with the manufacturer's specifications.

Acid Hydrolysis of Corneal Samples

Post DSC analysis, the tissue was recovered and dried, and dry-weight was recorded. To stabilize the Schiff bases contained in the difunctional cross-links, dried samples were reduced with $NaBH_4$ (reagent/sample weight ratio of 1:30) for 1 hour at room temperature. The reduced samples were then washed with water twice, dried, and hydrolyzed with 6N HCl in vacuo for 18 hours at 110°C after argon sparging. The hydrolysates were dried to evaporate HCl, reconstituted with H_2O, and re-dried to remove residual HCl. After the last washing step, hydrolysate was reconstituted with H_2O. An aliquot was then taken for OH-pro analysis.

Cross-Link Enrichment and LC/MS

Post hydrolysis, cross-link enrichment was carried out by using a cellulose mini-column method (Bond-Elut cellulose Agilent part No. 168726; Agilent Technologies, Inc., Santa Clara, CA, USA). The cellulose column was equilibrated with organic mobile phase (ACN:AcOH:H_2O [8:1:1]). The dried hydrolysate was dissolved in ACN:AcOH (6:1) mixture and applied on equilibrated cellulose column. The column was flushed with 12 mL organic mobile phase to remove most of the free amino acids and residual acid. The cross-links were then eluted with water, collected, and dried in preparation for HPLC analysis. An internal standard, acetyl-PYD, was added post hydrolysis and pre cellulose in order to account for any losses during the enrichment step.

Having these standards allowed us to build accurate, reproducible, calibration curves and we recalibrated on a weekly basis. In addition, the guard column was changed frequently to help ensure consistent results. Calibration curves were prepared by injecting standards at seven concentrations ranging from 0 to 180 pmol DHLNL, 0 to 130 pmol HLNL, 0 to 200 pmol LNL, 0 to 116 pmol HHL, 0 to 24 pmol PYD, 0 to 10.7 pmol DPYD, 0 to 209 pmol DES/IDE, and 0 to 146 pmol Pent. The calibration curve of each compound was described by the linear equation, with coefficient (r^2) of the curve > 0.995 for all the compounds.

Cellulose-enriched cross-links were analyzed on a LC/MS system consisting of an Agilent 1100 HPLC with UV/visible diode array/fluorescence/mass (DAD/FLD/MSD) detectors (Chemstation Rev.B.03.01). The mobile phase was an isocratic, degassed 20 mM HFBA/MeOH mixture (70:30), with a flow rate of 1 mL/min. Eclipse XDB-C8 column (4.6 mm × 250 mm) was used with operating temperature of 25°C using the column oven. A tee fitting was introduced after the DAD in order to direct 80% flow to the FLD and 20% to the MSD. Thus, a pump flow rate of 1 mL/min resulted in a 0.2 mL/min flow rate to the MSD. Using selected ion monitoring allowed for greater sensitivity, and the following target ions were measured: DHLNL ($m/z = 308.2$), HLNL ($m/z = 292.2$), LNL ($m/z = 276.1$), HHL ($m/z = 445.2$), PYD ($m/z = 429.2$), DPYD ($m/z = 413$), DES/IDE ($m/z = 526.3$), and Pent ($m/z = 379.2$). Running the FLD in parallel to the MSD allowed for an additional quality control measure, since the fluorescence signals are well characterized for collagen cross-links such as the pyridinolines (ex295/em395) and the nonenzymatic glycation– and age-associated cross-link Pent (ex335/em385), and as such, can be readily compared to the expected MSD signal abundances. The relevant chromatograms were extracted by using Chemstation software and the abundance measurements were converted into picomoles by using the programmed calibration table. The cross-link densities were then determined for each cross-link relative to collagen content, which is determined colorimetrically by the method described in the Hydroxyproline Analysis Assay section, and expressed in mol/mol quantity. Each sample was injected three times and we obtained a collagen cross-link profile from every sample.

Hydroxyproline Analysis Assay

The following was adopted from previously reported procedures.[28–30] Stock buffer (10X): 50 g citric acid monohydrate, 12 mL glacial AcOH, 120 g sodium acetate trihydrate, 34 g NaOH were made up to a final volume of 1L distilled water. The pH was adjusted to 6 and the buffer was stored at 4°C until use. Stock buffer was diluted 10X to prepare assay buffer (1X). The following reagents were prepared freshly on the day of the experiment: OH-pro standard, Chloramine-T reagent, and 4-(dimethylamino) benzaldehyde (DMBA) reagent. The OH-pro standard was prepared by dissolving dried L–OH-pro with assay buffer to the appropriate concentrations (0–10 μg/mL). Chloramine-T reagent was prepared by dissolving 0.3525 g Chloramine-T powder in 5.175 mL H_2O, with 6.5 mL n-propanol and 13.325 mL stock buffer. The DMBA mixture was made by dissolving 3.75 g DMBA in 15 mL n-propanol and 6.5 mL perchloric acid. Appropriate dilutions of standard OH-pro solution (0–10 μg/mL) and hydrolysate (1:50, 1:100, or 1:250) were prepared by using assay buffer. After aliquoting 200 μL standard OH-pro solution and diluted hydrolysate into tubes, 100 μL Chloramine-T reagent was added, gently pipetted to mix, and incubated at room temperature for 20 minutes. One hundred microliters of DMBA reagent was then added to each sample, gently mixed, and the chromophore was developed by incubating the sample at 60°C for 15 minutes. Immediately after the incubation, absorbance of each sample was measured at 540 nm by using a spectrophotometer (ELx800; Bio-Tek Instruments, Inc., Winooski, VT, USA). The total collagen content for each sample was calculated by assuming 14% OH-pro content per collagen by weight and using 300 kDa for the molecular weight of the collagen molecule.[2]

Statistical Analysis

Statistical analysis was carried out with the assistance of the Biostatistics Consulting Service of the Irving Center for Clinical Trials at Columbia University Medical Center. All quantitative data (mean ± SD) including all ages combined were assessed for significance initially by using Student's *t*-test. This was followed by a stratified analysis comparison within the age groups, ≤40 years and >40 years (a stratified analysis). The results from both *t*-tests and Wilcoxon rank sum tests were in

Investigative Ophthalmology & Visual Science

Table. Summary of Analysis of KC Versus Control for All Ages Combined, Age ≤ 40 Years and > 40 Years

	All Ages Combined					Age ≤ 40 y					Age > 40 y				
	n	Mean	±	SD	*P*	*n*	Mean	±	SD	*P*	*n*	Mean	±	SD	*P*
T_m, °C															
Control	10	60.08	±	1.54	0.12	4	61.40	±	0.56	**0.00**	8	59.19	±	1.31	0.68
KC	15	59.21	±	1.16		6	58.94	±	0.73		7	59.53	±	1.52	
Hydration status (water content), %															
Control	11	75	±	3	0.39	5	73	±	3	**0.00**	8	76	±	3	**0.01**
KC	17	72	±	12		6	82	±	4		9	64	±	11	
Collagen content, %															
Control	11	45	±	5	0.48	5	48	±	4	0.43	8	42	±	5	0.09
KC	17	47	±	7		6	45	±	8		9	48	±	7	
Total cross-link, mol/mol collagen															
Control	11	0.323	±	0.088	0.50	5	0.313	±	0.113	0.38	8	0.333	±	0.071	0.97
KC	17	0.297	±	0.104		6	0.255	±	0.107		9	0.335	±	0.092	
DHLNL, mol/mol collagen															
Control	11	0.048	±	0.024	**0.03**	5	0.032	±	0.022	0.06	8	0.062	±	0.019	0.06
KC	17	0.074	±	0.031		6	0.055	±	0.018		9	0.091	±	0.031	
HLNL, mol/mol collagen															
Control	11	0.043	±	0.005	0.68	5	0.041	±	0.007	0.69	8	0.045	±	0.004	0.36
KC	17	0.045	±	0.015		6	0.038	±	0.011		9	0.050	±	0.016	
LNL, mol/mol collagen															
Control	11	0.190	±	0.055	**0.02**	5	0.185	±	0.057	**0.04**	8	0.194	±	0.059	0.20
KC	17	0.132	±	0.063		6	0.114	±	0.052		9	0.148	±	0.070	
HHL, mol/mol collagen															
Control	11	0.042	±	0.030	0.70	5	0.055	±	0.037	0.77	8	0.032	±	0.022	0.19
KC	17	0.047	±	0.030		6	0.048	±	0.042		9	0.046	±	0.017	

Statistically significant *P* values are indicated in bold.

good agreement. For the skewed data, *t*-tests were done with log-transformed values. Statistical significance of all tests was based on an α value of 0.05 ($P < 0.05$). Owing to the small sample numbers, multiple comparison adjustments were not considered relevant for this study.

Analysis of LC/MS Data With T_m as Determined by DSC

Data from the LC/MS cross-link analysis were correlated with T_m by using data as reported in the accompanying report in order to assess whether individual or total cross-link levels correlated with fibril thermal stability. Correlation coefficients for each cross-link as a function of T_m were determined by using Microsoft Excel (version 14.0; Microsoft Corporation, Redmond, WA, USA).

Results

The results for hydration, collagen content, T_m for all groups and for age ≤ 40 years and age > 40 years are shown in the Table.

Before the LC/MS sample preparation, T_m, water content, and collagen content of each sample were determined. Thermal denaturation temperature was measured to determine the fibril stability of each sample. Water content was measured to determine the hydration status of the tissue, and collagen content was measured colorimetrically (OH-pro assay), in order to express the cross-link levels on a mole/mole basis.

Thermal Denaturation Temperature

Thermal denaturation temperature of each sample was measured by using DSC and the results of thermal denaturation testing are shown in Figure 2A. The average T_m of controls and KC corneas did not show significant difference (60.08 ± 1.54 vs. 59.21 ± 1.16, $P = 0.12$). Since KC progression is known to be more severe in the younger population,[31] the samples were divided into two groups: age ≤ 40 years and age > 40 years. Compared with the control, the KC ≤ 40 group had lower T_m values, indicating less fibril stability (61.40 ± 0.56, 58.94 ± 0.73, $P = 0.0002$). This is an approximate 2.5°C difference between KC ≤ 40 and controls. This amount of change in T_m can be achieved by using the CXL methods[32] as well as other chemical topical approaches.[33] Interestingly, the older control samples had a significant decrease in T_m as compared to the younger control samples. Such a trend has also been reported previously albeit it has not been well studied.[34,35] With regard to T_m for many other tissues, the T_m generally increases with aging and this is generally believed to be as a result of age-related nonenzymatic cross-linking. This is true for tendon,[36] skin,[37,38] cartilage,[39] blood vessel,[40] and other tissues.

Tissue Hydration

Hydration status of corneal samples was determined by calculating percentage water content in each sample (Fig. 2B). The hydration status of controls and KC corneas was not significantly different (75% ± 3% vs. 72% ± 12%, $P = 0.39$). However, KC ≤ 40 samples were slightly more hydrated (swollen) as compared to those of controls ≤ 40 (82% ± 4%

Investigative Ophthalmology & Visual Science

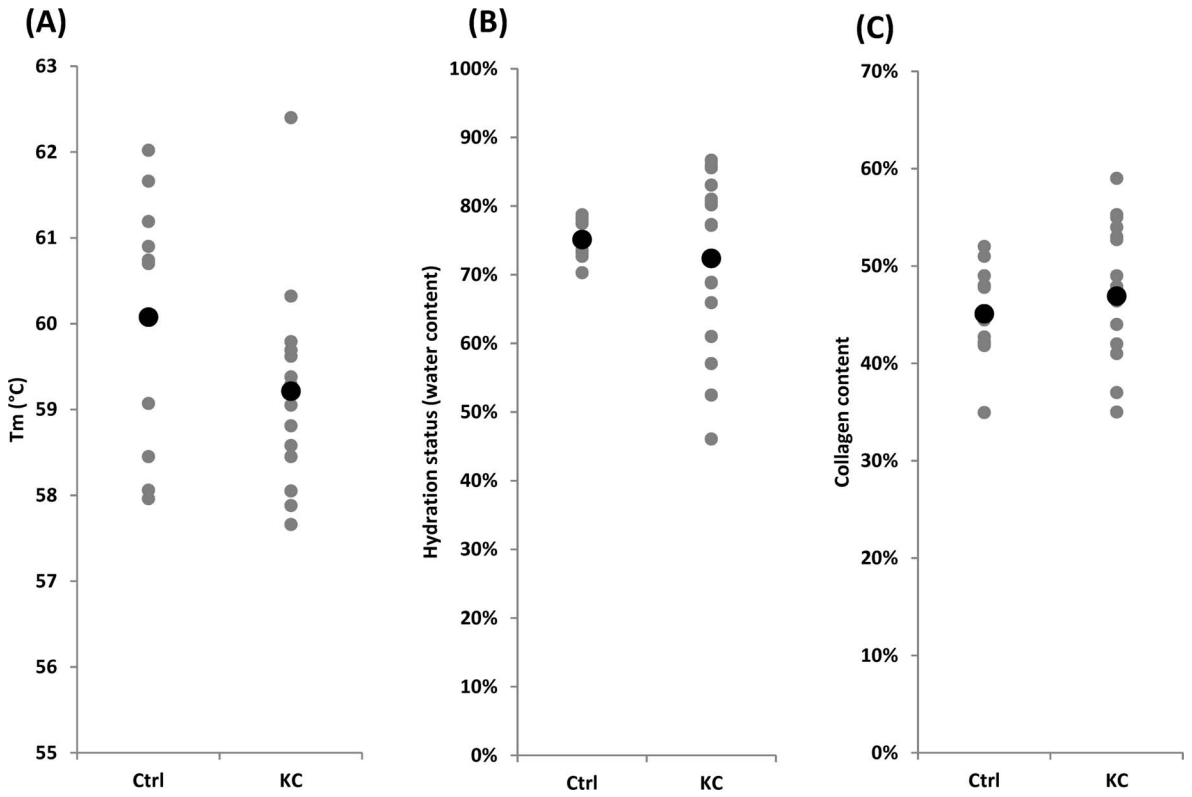

FIGURE 2. Comparison of human KC versus Eye-Bank controls for (**A**) average T_m, (**B**) average tissue hydration (% water content), and (**C**) average collagen content (%). *Black dots* represent the mean values, and *gray dots* represent the actual values measured. In each case, comparisons were made between controls and KC by using Student's *t*-test. Statistically significant difference was not detected.

vs. 73% ± 3%, $P = 0.0013$). On the other hand, KC > 40 samples were slightly more dehydrated than those of controls (64% ± 11% vs. 76% ± 3%, $P = 0.01$). Water content of control ≤ 40 and control > 40 samples were 73% ± 3% and 76% ± 3%, respectively, which was in good agreement with previously reported hydration status of corneal tissue.[41] It is known that the hydration status affects the shift in denaturation temperature. Considering that the older KC samples were relatively dehydrated compared to the older control samples, the observed T_m of older KC corneas could have been slightly higher than it was at normal hydration status.[42] The KC ≤ 40 samples were slightly more hydrated than control ≤ 40 samples, which could mean that the observed T_m was artificially lowered owing to the extra water in the sample. However, in our experience, this level of difference in hydration will not produce a significant shift in T_m. It is not clear whether the hydration could be responsible for the observed ~2°C shift in the thermal denaturation temperature between the KC ≤ 40 and control corneas.

Collagen Content

Figure 2C shows the result of collagen content analysis by OH-pro assay. The levels varied from approximately 35% to 59%, which was lower than values reported in the literature.[43,44] There was no notable difference in average collagen content between controls and KC corneas (45% ± 5% vs. 47% ± 7%, $P = 0.48$). Collagen content of younger populations in control and KC was not particularly different (48% ± 4% vs. 45% ± 8%, $P = 0.43$). Thus, our results regarding collagen content are essentially in agreement with previous reports and indicate that collagen content per se likely is not a key consideration in KC pathogenesis.[43] It is more likely that qualitative collagen changes underlie mechanical instability.

Cross-Linking Evaluation

Figures 1A and 1B show the nine cross-link compounds that were measured, and the elution profile of the standard cross-link compounds, by using LC/MS. Selective ion monitoring mode (details described in the Materials and Methods section) was used in order to optimize signal strength. Of all the nine cross-links, DHLNL, HLNL, LNL, and HHL were detected in both KC and control corneas.

Figure 3A summarizes the detected cross-link density expressed relative to the collagen content of each sample (mol/mol collagen). One of the major findings of this analysis was that LNL was the dominant difunctional cross-link in human cornea. Furthermore, compared to the controls, KC corneas contained fewer LNL molecules with the average values of 0.132 ± 0.063 vs. 0.190 ± 0.055 ($P = 0.02$). The level of DHLNL on the other hand was slightly increased in KC (0.074 ± 0.031 vs. 0.048 ± 0.024, $P = 0.03$). When the samples were divided by age groups, it was found that LNL had the same trend in KC ≤ 40 versus control (0.114 ± 0.052 vs. 0.185 ± 0.057, $P = 0.04$). For DHLNL, however, the trend was not seen in either age group (Table).

Regarding HLNL and HHL, the levels were not significantly different between KC and control (HLNL: 0.045 ± 0.015 vs. 0.043 ± 0.005, $P = 0.68$; HHL: 0.047 ± 0.030 vs. 0.042 ± 0.030, $P = 0.70$). Of note, HHL has been shown to be derived from an unreduced form of HLNL (i.e., deH-HLNL) in skin and cornea. This deH-HLNL matures into a trifunctional stable cross-link, HHL, by reacting with histidine[11,12,45,46]; therefore, HLNL and HHL tend to have an inverse relationship, with HLNL

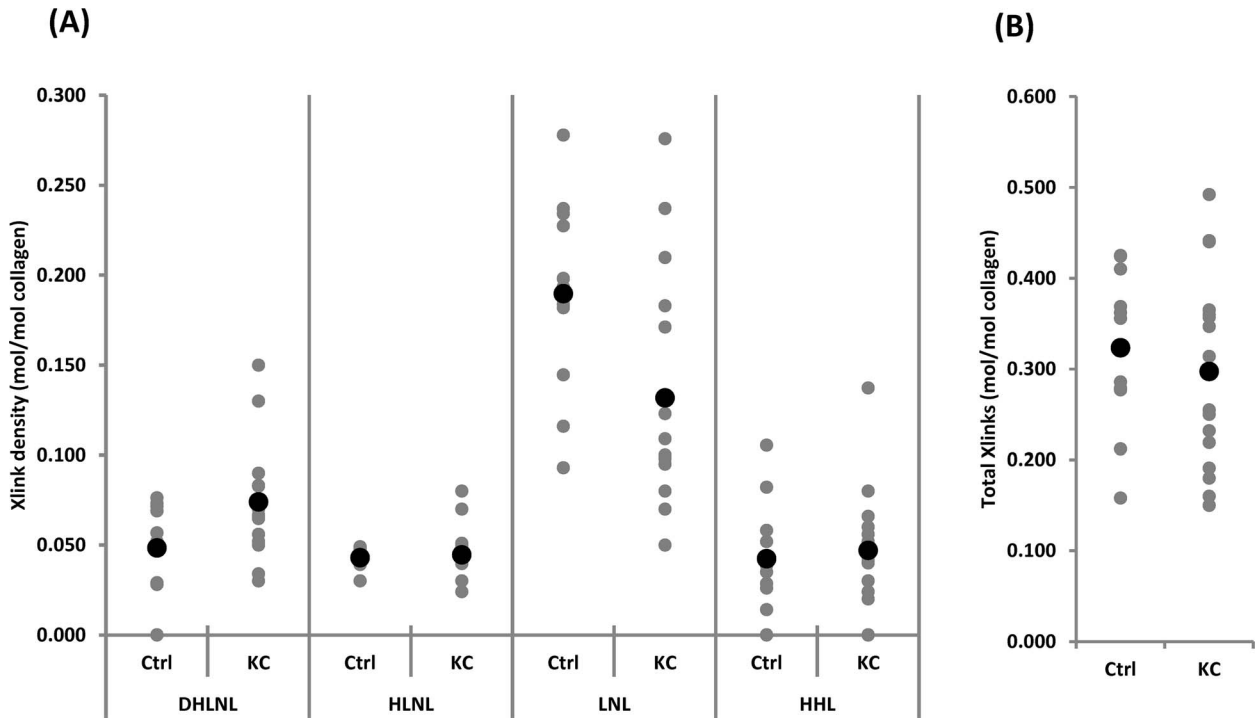

FIGURE 3. (**A**) Levels of specific di- and trifunctional corneal CTP cross-links in samples detected by LC/MS and (**B**) the sum of all the cross-links detected in each groups. *Black dots* represent the mean values and *gray dots* represent the actual values measured. See Materials and Methods for procedural details. Comparisons were made between controls and KC by using Student's *t*-test. Statistically significant difference was detected in DHLNL and LNL levels ($P < 0.05$).

being higher when HHL is lower, and vice versa. In our study, we did not observe such a relationship. To the best of our knowledge, this was the first attempt to measure HHL in KC samples. Our levels were somewhat lower than those previously reported by Yamauchi et al.[11] for HHL in normal bovine cornea. However, because the chromatographic and detection methods were quite different, it is difficult to draw direct comparisons.

Regarding other cross-links included in the analysis, we did not detect levels of either PYD or DPYD in any of our samples. This was consistent with previous reports showing that both of these trifunctional collagen cross-links are absent in corneal tissue.[47] The tetrafunctional cross-links DES and IDE result from a spontaneous condensation of two adjacent LNL difunctional cross-links in the elastin molecule, which has a unique primary sequence involving adjacent lysine residues that allow for intermolecular difunctional LNL formation followed by the desmosine-resulting condensation.[48] Desmosines have not been previously detected in corneal tissue and our findings are in agreement with this. Previous studies using a two-step HPLC method have found the nonenzymatic glycosylation cross-link Pent to be increased in the diabetic human cornea.[49] We did not detect Pent, however, in either KC samples or controls, and the reason for this discrepancy with prior studies is not completely clear but may relate to the differences in the analytic techniques used.

Figure 3B shows the total cross-link density (sum of all the cross-links) of control and KC samples. There was no significant difference between KC and control (0.297 ± 0.104 vs. 0.323 ± 0.088, $P = 0.5$). The younger populations that are considered to have the severe forms of KC did not differ in their total cross-link density when compared to the controls. This suggests that rather than the overall cross-link density, there might be a particular cross-link (such as LNL) that holds the key to fibril instability.

Cross-Link Density Versus T_m

To determine if there was a direct correlation between fibril stability and either total cross-link density or any specific cross-links, we created scatterplots of cross-link density as a function of T_m (Fig. 4). Lower T_m in KC corneas indicates fibril instability. There was not a statistically significant correlation between T_m and total cross-link density (Fig. 4) or the density of individual specific cross-links (data not shown). Thus, the fibril thermal stability changes were not directly attributable to any of the individual cross-links examined or in total. This suggests that other causes of fibril instability may exist, including as yet unidentified cross-links.

DISCUSSION

Thermal denaturation temperature (also known as thermal shrinkage temperature), has been used in the evaluation of a variety of collagenous tissues for many decades. It has been a mainstay in the biomaterials industry along with various mechanical testing modalities.[50] Evaluation of T_m is well suited to collagenous tissues, since collagen molecules in a fibril undergo a largely "cooperative" or coordinated denaturation, producing a prominent, well-defined, endotherm.[51] Although this technique has been used in many other tissues, very little published literature exists on thermal denaturation of the cornea,[52–55] and only two reports have considered age-related changes in T_m of human cornea: one by Stringer and Parr[34] in 1964 and the other by Chang et al.[35] in 1996.[·] Both have found that T_m decreases with increasing age. In general, the opposite effect is seen with other tissues such as tendon and skin, in which T_m increases with aging.[36] This is thought to be due to the accumulation of nonenzymatic cross-links with age. The reason for this opposite finding in corneal tissue is not clear. However, we did not detect the age-related nonenzymatic

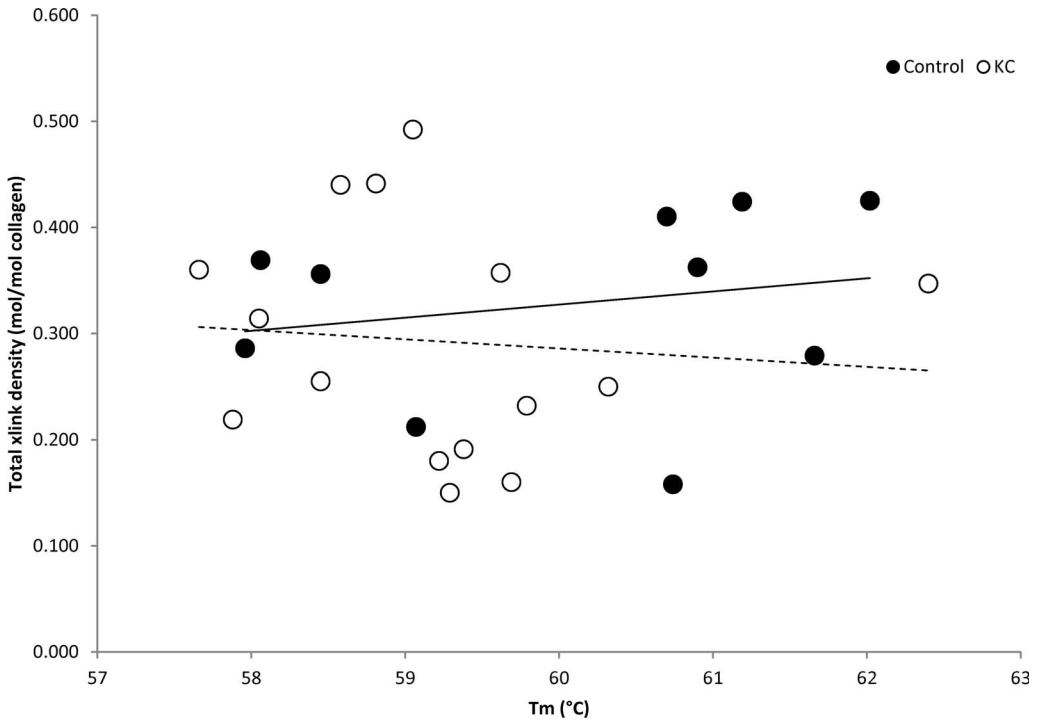

FIGURE 4. Analysis of total cross-link density (mol/mol collagen) as a function of T_m for control (*black circle*) and KC (*open circle*) samples. The trend lines are expressed with a *solid line* (control) and a *dotted line* (KC). There was no statistical significant correlation between fibril stability and the cross-link density.

cross-link Pent in our samples, suggesting that age-related corneal cross-linking was not significant in our samples.

Because corneal tissue is so largely made up of collagenous proteins, the major peak is a valid measure of collagen fibril denaturation that occurs during the unwinding of molecular triple helices.[51] We have previously used a related, albeit cruder, method of measuring the same properties, known as thermal shrinkage temperature analysis.[56] Thermal denaturation can be used to determine differences in the degree of induced cross-linking in tissues treated with CXL[32] or chemical agents[56] (i.e., glutaraldehyde, formaldehyde, genipin, glyceraldehyde, formaldehyde releasers)[50] and has been used to study changes in cross-linking in studies related to aging as well as modulation of enzymatic cross-linking.[51] Of note, thermal denaturation of lens capsule tissue is unaffected by proteoglycan removal using guanidine but is disrupted by collagenase digestion,[57,58] indicating that the primary determinant of the T_m is not proteoglycans but collagenous structures.

Difunctional cross-links in human KC tissue have been measured previously in three separate reports.[22–24] Unfortunately, because the methods used at that time are quite different from that of the present study using LC/MS, it is not possible to draw direct comparisons. Furthermore, the results are conflicting among the three studies. Quantitation in those studies uses scintillation counting and is reported as a rate in counts per minute, making unit conversions into mol/mol not possible. The HHL densities in mol/mol units have been reported by Yamauchi et al.[11,12] in bovine skin and cornea. The HHL levels in the present study were lower than those previously reported. Again, it is difficult to make direct comparisons because the detection methods were dissimilar (i.e., chemical derivatization and UV/visible light detection).

The initial attempt to measure difunctional enzymatic cross-links in KC was reported in 1978 by Cannon and Foster,[22] at which time the investigators suggested that KC patients' corneas contain higher levels of LNL. However, opposite findings have been reported in follow-up studies carried out in 1985 and 1988[23,24]; HHL, a major nonreducible trifunctional cross-link, was not included in any of these studies, as the methods for detection were not available at that time. Our results provide additional information to the corneal chemical cross-link analysis literature. Our results regarding LNL support the original study by Cannon and Foster.[22]

We were particularly interested in seeing how levels of HHL, a major trifunctional cross-link found in cornea and skin but not in sclera or tendon, may be altered in KC. Because HHL is derived from HLNL, a functional impairment or deficiency of LOX could result in lower levels of HLNL and by extension, HHL. On the premise that LOX or LOXL enzymes are altered in KC, we expected to see such changes, but did not.

In our study, it was interesting to find an inverse relationship between DHLNL and LNL levels. The determinant of whether the collagen fibrils form DHLNL or LNL is governed by LOX and/or lysyl hydroxylase. Lysyl hydroxylase is responsible for hydroxylation of lysine residues. LOX catalyzes the oxidative deamination of lysine and hydroxylysine residues. Our findings support the possibility that the activity of LOX and/or lysyl hydroxylase is involved in the pathogenesis of KC.

Lysinonorleucine is an important difunctional connective tissue protein cross-link that is found not only in collagenous proteins but also in elastin. Although previously considered to be absent from corneal tissue, recent evidence from Kamma-Lorger and others[59] suggests that an extensive network of elastin-resembling microfibrils exists in the human cornea and is particularly conspicuous in the posterior cornea. That is, elastin or a similar protein (i.e., oxytalan, fibrillin) is present, particularly in the posterior corneal layers.[59–62] Lysinonorleucine is a difunctional cross-link that is a condensation of two lysine moieties without hydroxylation. A deficiency in LNL in KC tissue thus could represent diminished cross-linking either in fibrillar collagen or possibly an elastic precursor protein such as oxytalan (also known as fibrillin). Significant literature

related to fibrillin-1 and fibrillin-2 is available.[63–65] There are three major possibilities for cross-linking defects in the fibrillin molecule:

1. Disulfide linkages (not enzyme mediated)—Fibrillin is the most cysteine-rich protein known. Its initial assembly is initiated by disulfide bond formation[66];
2. Transglutaminase and formation of γ-glutamyl-lysine cross-links—In addition to the findings by Qian and Glanville[67] from 1997 that alignment of fibrillin molecules in elastic microfibrils is defined by transglutaminase-derived cross-links, a tropoelastin-fibrillin-transglutaminase–mediated cross-link has been identified as being a critical interaction[64]; and
3. LOX and LOXL-derived LNL precursor aldimine Schiff base and desmosine—Although the appearance of desmosines from the formation of two adjacent LNL Schiff base precursors has been well described for elastin,[68] the identification of difunctional LNL Schiff base precursors specifically in fibrillin microfibrillar protein is not well known, to the best of our knowledge.

Cross-linking for both collagen and elastin processes are mediated by LOX and its related subtypes, namely, LOXL-1 to LOXL-4.[69,70] The precise substrate specificity for LOX and the four LOXL enzymes is not completely known. However, LOX and LOXL-1 are known to be involved in elastin cross-linking.[71] In addition, hydroxylation can also play a key role in pathogenesis by determining which difunctional cross-links form preferentially.[3]

Although the findings from this study support the genetic and immunohistochemical study findings that a LOX deficiency underlies pathogenesis, we acknowledge several limitations. First, we compared specimens obtained from three types of lamellar keratoplasty (ALK, DALK, and PKP) to full-thickness corneal buttons obtained post mortem from the eye bank. Most of our surgical tissue samples were from ALK or DALK; ALK generally includes the anterior 25% to 50% of the cornea, while DALK includes 90% to 95% of the corneal thickness. There are known differences in mechanical properties between anterior and posterior corneal lamellae, including increased interweaving anteriorly with a more orthogonal orientation posteriorly.[72–77] Depth-dependent differences in enzymatic cross-link levels could be present and represent a limitation of this study. In future studies, we will address this potentially important issue by determining regional and depth-dependent differences in cross-link levels. Second, as these were surgical specimens, they represented the most advanced KC cases and therefore may not reflect well the cross-links present during the early progression of disease. That is why we chose to focus on the younger group (age $\leq$ 40 years) for associations related to pathogenesis because these younger patients would be more likely to show an earlier state of disease.[31] Many of the patients had developed scarring from contact lens wear, thus clearly entering into a damage-repair cycle that may not fully reflect native collagen protein cross-link chemistry.

In the present study we evaluated chemical collagen and elastin cross-links as well as the T_m of surgical KC specimens. Our results indicate that fibril stability was reduced in KC samples below the age of 40 years. In addition, the difunctional cross-link LNL is the primary difunctional cross-link in the human cornea, and the levels were reduced in KC samples as compared to controls. We also measured HHL in KC samples for the first time.

Acknowledgments

The authors wish to thank Simon P. Robins, PhD, for providing HHL and HLNL standards, and the Biostatistics Consulting Service of the Irving Center for Clinical Trials at Columbia University Medical Center for biostatistical consultation.

Supported in part by Research to Prevent Blindness, National Institutes of Health Grants National Center for Research Resources (NCRR) UL1RR024156, National Eye Institute (NEI) P30 EY019007, and NEI R01EY020495 (DCP), and the Bjorg & Stephen Ollendorf Fund.

Disclosure: **A. Takaoka**, None; **N. Babar**, None; **J. Hogan**, None; **M. Kim**, None; **M.O. Price**, None; **F.W. Price Jr**, None; **S.L. Trokel**, None; **D.C. Paik**, None

References

1. Meek KM, Hayes S. Corneal cross-linking: a review. *Ophthalmic Physiol Opt*. 2013;33:78–93.
2. Avery NC, Sims TJ, Bailey AJ. Quantitative determination of collagen cross-links. *Methods Mol Biol*. 2009;522:103–121.
3. Eyre DR, Weis MA, Wu JJ. Advances in collagen cross-link analysis. *Methods*. 2008;45:65–74.
4. Robins SP. Biochemistry and functional significance of collagen cross-linking. *Biochem Soc Trans*. 2007;35:849–852.
5. Marcovich AL, Brandis A, Daphna O, et al. Stiffening of rabbit corneas by the bacteriochlorophyll derivative WST11 using near infrared light. *Invest Ophthalmol Vis Sci*. 2012;53:6378–6388.
6. Garcia-Castineiras S, Dillon J, Spector A. Detection of bityrosine in cataractous human lens protein. *Science*. 1978; 199:897–899.
7. Dyer DG, Blackledge JA, Thorpe SR, Baynes JW. Formation of pentosidine during nonenzymatic browning of proteins by glucose: identification of glucose and other carbohydrates as possible precursors of pentosidine in vivo. *J Biol Chem*. 1991; 266:11654–11660.
8. Kagan HM, Trackman PC. Properties and function of lysyl oxidase. *Am J Respir Cell Mol Biol*. 1991;5:206–210.
9. Trackman PC. Diverse biological functions of extracellular collagen processing enzymes. *J Cell Biochem*. 2005;96:927–937.
10. Yamauchi M, Sricholpech M. Lysine post-translational modifications of collagen. *Essays Biochem*. 2012;52:113–133.
11. Yamauchi M, Chandler GS, Tanzawa H, Katz EP. Cross-linking and the molecular packing of corneal collagen. *Biochem Biophys Res Commun*. 1996;219:311–315.
12. Yamauchi M, London RE, Guenat C, Hashimoto F, Mechanic GL. Structure and formation of a stable histidine-based trifunctional cross-link in skin collagen. *J Biol Chem*. 1987; 262:11428–11434.
13. Bykhovskaya Y, Li XH, Epifantseva I, et al. Variation in the lysyl oxidase (LOX) gene is associated with keratoconus in family-based and case-control studies. *Invest Ophthalmol Vis Sci*. 2012;53:4152–4157.
14. Dudakova L, Liskova P, Trojek T, Palos M, Kalasova S, Jirsova K. Changes in lysyl oxidase (LOX) distribution and its decreased activity in keratoconus corneas. *Exp Eye Res*. 2012;104:74–81.
15. Li XH, Bykhovskaya Y, Haritunians T, et al. A genome-wide association study identifies a potential novel gene locus for keratoconus, one of the commonest causes for corneal transplantation in developed countries. *Hum Mol Genetics*. 2012;21:421–429.
16. Akhtar S, Bron AJ, Salvi SM, Hawksworth NR, Tuft SJ, Meek KM. Ultrastructural analysis of collagen fibrils and proteoglycans in keratoconus. *Acta Ophthalmol*. 2008;86:764–772.
17. Shore RC, Moxham BJ, Berkovitz BKB. Changes in collagen fibril diameters in a lathyritic connective-tissue. *Connect Tissue Res*. 1984;12:249–255.

18. Sawaguchi S, Fukuchi T, Abe H, Kaiya T, Sugar J, Yue BYJT. Three-dimensional scanning electron microscopic study of keratoconus corneas. *Arch Ophthalmol*. 1998;116:62–68.
19. Kenney MC, Nesburn AB, Burgeson RE, Butkowski RJ, Ljubimov AV. Abnormalities of the extracellular matrix in keratoconus corneas. *Cornea*. 1997;16:345–351.
20. Pouliquen Y, Faure JP, Limon S, Bisson J. Extracellular deposits of corneal stroma in keratoconus: electron microscopic study [in French]. *Arch Ophtalmol Rev Gen Ophtalmol*. 1968;28: 283–294.
21. Andreassen TT, Simonsen AH, Oxlund H. Biomechanical properties of keratoconus and normal corneas. *Exp Eye Res*. 1980;31:435–441.
22. Cannon DJ, Foster CS. Collagen crosslinking in keratoconus. *Invest Ophthalmol Vis Sci*. 1978;17:63–65.
23. Oxlund H, Simonsen AH. Biochemical studies of normal and keratoconus corneas. *Acta Ophthalmol (Copenh)*. 1985;63: 666–669.
24. Critchfield JW, Calandra AJ, Nesburn AB, Kenney MC. Keratoconus: I, biochemical studies. *Exp Eye Res*. 1988;46: 953–963.
25. McCall AS, Kraft S, Edelhauser HF, et al. Mechanisms of corneal tissue cross-linking in response to treatment with topical riboflavin and long-wavelength ultraviolet radiation (UVA). *Invest Ophthalmol Vis Sci*. 2010;51:129–138.
26. Kato Y, Uchida K, Kawakishi S. Aggregation of collagen exposed to UVA in the presence of riboflavin: a plausible role of tyrosine modification. *Photochem Photobiol*. 1994;59:343–349.
27. Gineyts E, Borel O, Chapurlat R, Garnero P. Quantification of immature and mature collagen crosslinks by liquid chromatography-electrospray ionization mass spectrometry in connective tissues. *J Chromatogr B Analyt Technol Biomed Life Sci*. 2010;878:1449–1454.
28. Woessner JF. Determination of hydroxyproline in tissue and protein samples containing small proportions of this imino acid. *Arch Biochem Biophys*. 1961;93:440–447.
29. Stegemann H, Stalder K. Determination of hydroxyproline. *Clin Chim Acta*. 1967;18:267–273.
30. Reddy GK, Enwemeka CS. A simplified method for the analysis of hydroxyproline in biological tissues. *Clin Biochem*. 1996; 29:225–229.
31. Ertan A, Muftuoglu O. Keratoconus clinical findings according to different age and gender groups. *Cornea*. 2008;27:1109–1113.
32. Spoerl E, Wollensak G, Dittert DD, Seiler T. Thermomechanical behavior of collagen-cross-linked porcine cornea. *Ophthalmologica*. 2004;218:136–140.
33. Babar N, Kim M, Cao K, et al. Cosmetic preservatives as therapeutic corneal and scleral tissue cross-linking agents. *Invest Ophthalmol Vis Sci*. 2015;56:1274–1282.
34. Stringer H, Parr J. Shrinkage temperature of eye collagen. *Nature*. 1964;204:1307.
35. Chang J, Soderberg PG, Denham D, Nose I, Parel JM. Quantification of temperature-induced corneal shrinkage. *Invest Ophthalmol Vis Sci*. 1996;37:303–303.
36. Labella FS, Paul G. Structure of collagen from human tendon as influenced by age and sex. *J Gerontol*. 1965;20:54–59.
37. Flandin F, Buffevant C, Herbage DA. Differential scanning calorimetry analysis of the age-related-changes in the thermal-stability of rat skin collagen. *Biochim Biophys Acta*. 1984;791: 205–211.
38. le Lous M, Flandin F, Herbage D, Allain JC. Influence of collagen denaturation on the chemorheological properties of skin, assessed by differential scanning calorimetry and hydrothermal isometric tension measurement. *Biochim Biophys Acta*. 1982;717:295–300.
39. Doman I, Illes T. Thermal analysis of the human intervertebral disc. *J Biochem Biophys Methods*. 2004;61:207–214.
40. Samouillan V, Dandurand J, Lacabanne C, et al. Analysis of the molecular mobility of collagen and elastin in safe, atheromatous and aneurysmal aortas. *Pathol Biol*. 2012;60:58–65.
41. Davson H. The hydration of the cornea. *Biochem J*. 1955;59: 24–28.
42. Miles CA, Avery NC, Rodin VV, Bailey AJ. The increase in denaturation temperature following cross-linking of collagen is caused by dehydration of the fibres. *J Mol Biol*. 2005;346:551–556.
43. Zimmermann DR, Fischer RW, Winterhalter KH, Witmer R, Vaughan L. Comparative studies of collagens in normal and keratoconus corneas. *Exp Eye Res*. 1988;46:431–442.
44. Bron AJ, Tripathi RC, Harding JJ, Crabbe MJC. Stromal loss in keratoconus. *Trans Ophthalmol Soc U K*. 1978;98:393–396.
45. Yamauchi M, Shiiba, M. Lysine hydroxylation and cross-linking of collagen. In: Kannicht C, ed. *Post-translational Modifications of Proteins, Tools for Functional Proteomics*. Totowa, NJ: Humana Press; 2008:95–108.
46. Mechanic GL, Katz EP, Henmi M, Noyes C, Yamauchi M. Locus of a histidine-based, stable trifunctional, helix to helix collagen cross-link: stereospecific collagen structure of type-I skin fibrils. *Biochemistry*. 1987;26:3500–3509.
47. Eyre DR, Paz MA, Gallop PM. Cross-linking in collagen and elastin. *Annu Rev Biochem*. 1984;53:717–748.
48. Bailey AJ. Molecular mechanisms of ageing in connective tissues. *Mech Ageing Dev*. 2001;122:735–755.
49. Sady C, Khosrof S, Nagaraj R. Advanced Maillard reaction and cross-linking of corneal collagen in diabetes. *Biochem Biophys Res Commun*. 1995;214:793–797.
50. Loke WK, Khor E. Validation of the shrinkage temperature of animal tissue for bioprosthetic heart valve application by differential scanning calorimetry. *Biomaterials*. 1995;16:251–258.
51. Xu Y. Thermal stability of collagen triple helix. *Methods Enzymol*. 2009;466:211–232.
52. Soergel F, Jean B, Seiler T, et al. Dynamic mechanical spectroscopy of the cornea for measurement of its viscoelastic properties in vitro. *Ger J Ophthalmol*. 1995;4:151–156.
53. Sporl E, Genth U, Schmalfuss K, Seiler T. Thermomechanical behavior of the cornea. *Ger J Ophthalmol*. 1997;5:322–327.
54. Ruberti JW, Melotti SA. Corneal and scleral collagens assessed by modulated differential scanning calorimetry. *Invest Ophthalmol Vis Sci*. 2004;45:U318–U318.
55. Sionkowska A. Thermal stability of UV-irradiated collagen in bovine lens capsules and in bovine cornea. *J Photochem Photobiol B*. 2005;80:87–92.
56. Paik DC, Wen Q, Braunstein RE, Airiani S, Trokel SL. Initial studies using aliphatic beta-nitro alcohols for therapeutic corneal cross-linking. *Invest Ophthalmol Vis Sci*. 2009;50: 1098–1105.
57. Bailey AJ, Sims TJ, Avery NC, Miles CA. Chemistry of collagen cross-links: glucose-mediated covalent cross-linking of type-IV collagen in lens capsules. *Biochem J*. 1993;296(pt 2):489–496.
58. Miles CA, Avery NC. Thermal stabilization of collagen in skin and decalcified bone. *Phys Biol*. 2011;8:1–12.
59. Kamma-Lorger CS, Boote C, Hayes S, et al. Collagen and mature elastic fibre organisation as a function of depth in the human cornea and limbus. *J Struct Biol*. 2010;169:424–430.
60. Alexander RA, Garner A. Oxytalan fibre formation in the cornea: a light and electron microscopical study. *Histopathology*. 1977;1:189–199.

Investigative Ophthalmology & Visual Science

61. Alexander RA, Garner A. Elastic and precursor fibres in the normal human eye. *Exp Eye Res*. 1983;36:305–315.
62. Carrington SD, Alexander RA, Grierson I. Elastic and related fibres in the normal cornea and limbus of the domestic cat. *J Anat*. 1984;139(pt 2):319–332.
63. Davis MR, Summers KM. Structure and function of the mammalian fibrillin gene family: implications for human connective tissue diseases. *Mol Genetics Metab*. 2012;107: 635–647.
64. Rock MJ, Cain SA, Freeman LJ, et al. Molecular basis of elastic fiber formation: critical interactions and a tropoelastin-fibrillin-1 cross-link. *J Biol Chem*. 2004;279:23748–23758.
65. Montes GS. Structural biology of the fibres of the collagenous and elastic systems. *Cell Biol Int*. 1996;20:15–27.
66. Reinhardt DP, Gambee JE, Ono RN, Bachinger HP, Sakai LY. Initial steps in assembly of microfibrils. Formation of disulfide-cross-linked multimers containing fibrillin-1. *J Biol Chem*. 2000;275:2205–2210.
67. Qian RQ, Glanville RW. Alignment of fibrillin molecules in elastic microfibrils is defined by transglutaminase-derived cross-links. *Biochemistry*. 1997;36:15841–15847.
68. Vrhovski B, Weiss AS. Biochemistry of tropoelastin. *Eur J Biochem*. 1998;258:1–18.
69. Noblesse E, Cenizo V, Bouez C, et al. Lysyl oxidase-like and lysyl oxidase are present in the dermis and epidermis of a skin equivalent and in human skin and are associated to elastic fibers. *J Invest Dermatol*. 2004;122:621–630.
70. Kagan HM, Sullivan KA. Lysyl oxidase: preparation and role in elastin biosynthesis. *Methods Enzymol*. 1982;82(pt A):637–650.
71. Liu X, Zhao Y, Gao J, et al. Elastic fiber homeostasis requires lysyl oxidase-like 1 protein. *Nat Genetics*. 2004;36:178–182.
72. Dias JM, Ziebarth NM. Anterior and posterior corneal stroma elasticity assessed using nanoindentation. *Exp Eye Res*. 2013; 115:41–46.
73. Last JA, Thomasy SM, Croasdale CR, Russell P, Murphy CJ. Compliance profile of the human cornea as measured by atomic force microscopy. *Micron*. 2012;43:1293–1298.
74. Morishige N, Wahlert AJ, Kenney MC, et al. Second-harmonic imaging microscopy of normal human and keratoconus cornea. *Invest Ophthalmol Vis Sci*. 2007;48:1087–1094.
75. Muller LJ, Pels E, Vrensen GF. The specific architecture of the anterior stroma accounts for maintenance of corneal curvature. *Br J Ophthalmol*. 2001;85:437–443.
76. Petsche SJ, Pinsky PM. The role of 3-D collagen organization in stromal elasticity: a model based on X-ray diffraction data and second harmonic-generated images. *Biomech Model Mechanobiol*. 2013;12:1101–1113.
77. Winkler M, Jester BE, Nien-Shy C, Chai D, Brown DJ, Jester JV. High resolution macroscopy (HRMac) of the eye using nonlinear optical imaging. *P Soc Photo Opt Ins*. 2010;7589.

Investigative Ophthalmology & Visual Science